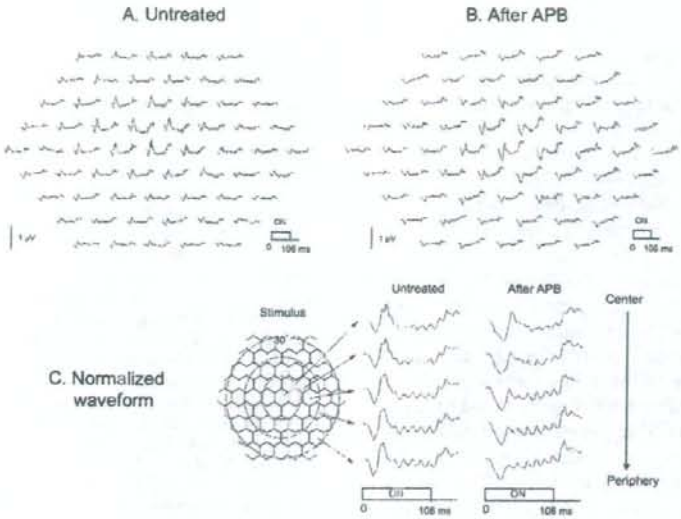

Fig. 4. Multifocal on- and off-responses before and after intravitreous injection of APB in a rhesus monkey. Intravitreous concentration of APB was 1.0 mM. Unstretched hexagonal elements (same size) are used for these monkey experiments. (A) Multifocal ERGs before APB. (B) Multifocal ERG after APB. (C) Normalized waveforms from five eccentric rings after APB application. The waveform after APB are very similar to those recorded from cCSNB patients.

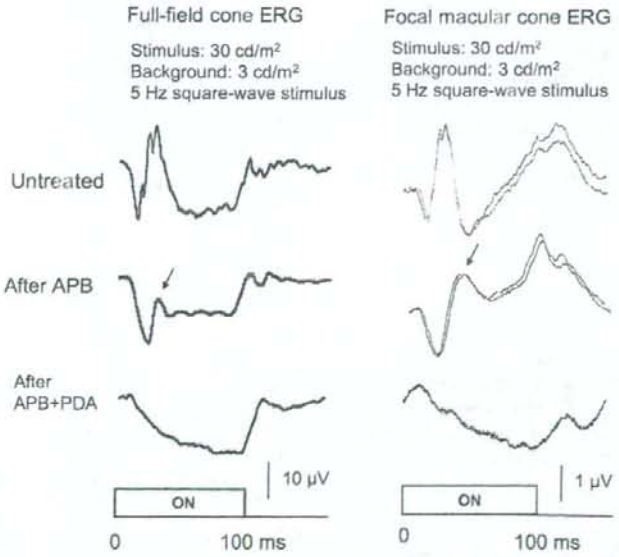

Fig. 5. Comparison in the waveforms of photopic ERG with long duration stimulus before and after APB and PDA application for full-field and focal macular cone ERGs in a rhesus monkey. Five hertz square-wave flickering stimulus of 30 cd/m² was presented on a background illumination of 3 cd/m² for both ERGs. After APB and PDA, the remaining positive wave at stimulus onset disappears completely for both ERGs (arrows).

APB-treated monkeys, the waveform of the d-wave at the offset of the stimulus was slightly different: the amplitude of the d-wave of the focal macular cone ERG was enhanced after the intravitreal injection of APB in monkeys, whereas the d-wave of focal macular cone ERG in cCSNB patients was not larger than that of myopic control. We do not know the reason for this difference in the waveform of the d-wave between the cCSNB patients and

APB-treated monkeys. However, it may be partly due to the differences between inherited human disease and the pharmacological animal model.

Although our electrophysiological study showed functional similarity between the retina of patients with cCSNB and APB-treated monkey retinas, there still remained the question of whether the retinal on-pathway is completely blocked in the retina of patients with cCSNB. Two psychophysical studies suggested that rod on-pathway may not be completely blocked in cCSNB patient (Allen et al., 2003; Young, Price, & Harrison, 1986).

We also found that even after a complete blockage of the cone on-pathway, there still remained a sizeable positive wave of the cone ERG in the central retina. The multifocal ERG results also demonstrated that the amplitude ratio of the positive wave to the a-wave was maximal in the central retina, and became gradually decreased towards the peripheral retina in a cCSNB patient and an APB-treated monkey supporting our combined findings of the full-field ERGs and focal macular cone ERGs. These results indicated that there is a unique spatial variation in the waveform of the cone ERGs. Other pharmacological studies in monkeys (Hare & Ton, 2002; Hood, Frishman, Saszik, & Viswanathan, 2002) also showed several spatial variations in the waveform of the cone ERGs using multifocal ERG technique, but they did not separate the on- and off-responses.

By adding PDA to APB, we found that the remaining positive wave of the cone ERG, which was seen even after blocking the cone on-pathway, originated from post-photoreceptor neurons which are sensitive to PDA, i.e., retinal neurons of the off-pathway or horizontal cells (Fig. 5). However, we could not identify exactly which retinal neurons/circuits contributed to this positive component. To identify the exact origin of this positive wave, further studies are needed using other pharmacological agents which affects specific retinal neurons.

Acknowledgments

The authors thank Laura J. Frishman of University of Huston for providing us her modified ophthalmoscope for multifocal ERG recordings for monkeys. We also thank Masao Yoshikawa, Eiichiro Nagasaka, Hidetaka Kudo of Mayo Corporation for technical helps.

References

Allen, L. E., Zito, I., Bradshaw, K., Patel, R. J., Bird, A. C., Fitzke, F., et al. (2003). Genotype-phenotype correlation in British families with X linked congenital stationary night blindness. *British Journal of Ophthalmology, 87*, 1413–1420.

Bech-Hansen, N. T., Naylor, M. J., Maybaum, T. A., Sparkes, R. L., Koop, B., Birch, D. G., et al. (2000). Mutations in NYX, encoding the leucine-rich proteoglycan nyctalopin, cause X-linked complete congenital stationary night blindness. *Nature Genetics, 26*, 319–323.

Dryja, T. P., McGee, T. L., Berson, E. L., Fishman, G. A., Sandberg, M. A., Alexander, K. R., et al. (2005). Night blindness and abnormal cone electroretinogram ON responses in patients with mutations in the GRM6 gene encoding mGluR6. *Proceedings of the National Academy of Sciences of the United States of America, 102*, 4884–4889.

Evers, H. U., & Gouras, P. (1986). Three cone mechanisms in the primate electroretinogram: Two with, one without OFF-center bipolar responses. *Vision Research, 26*, 245–254.

Hare, W. A., & Ton, H. (2002). Effects of APB, PDA, and TTX on ERG responses recorded using both multifocal and conventional methods in monkey. Effects of APB, PDA, and TTX on monkey ERG responses. *Documenta Ophthalmologica., 105*, 189–222.

Hood, D. C., Frishman, L. J., Saszik, S., & Viswanathan, S. (2002). Retinal origins of the primate multifocal ERG: Implications for the human response. *Investigative Ophthalmology & Visual Science, 43*, 1673–1685.

Houchin, K., Purple, R. L., & Wirtschafter, J. D. (1991). X-linked congenital stationary night blindness and depolarizing bipolar system dysfunction. [ARVO abstract]. *Investigative Ophthalmology & Visual Science, 32*, S1229 (Abstract No. 2741S).

Khan, N. W., Kondo, M., Hiriyanna, K. T., Jamison, J. A., Bush, R. A., & Sieving, P. A. (2005). Primate retinal signaling pathways: Suppressing ON-pathway activity in monkey with glutamate analogues mimics human CSNB1-NYX genetic night blindness. *Journal of Neurophysiology, 93*, 481–492.

Knapp, A. G., & Schiller, P. H. (1984). The contribution of on-bipolar cells to the electroretinogram of rabbits and monkeys. *Vision Research, 24*, 1841–1846.

Kondo, M., & Miyake, Y. (2000). Assessment of local cone on- and off-pathway function using multifocal ERG technique. *Documenta of Ophthalmologica, 100*, 139–154.

Kondo, M., Miyake, Y., Horiguchi, M., Suzuki, S., & Tanikawa, A. (1998). Recording multifocal electroretinogram on and off responses in humans. *Investigative Ophthalmology & Visual Science, 39*, 574–580.

Kondo, M., Miyake, Y., Kondo, N., Tanikawa, A., Suzuki, S., Horiguchi, M., et al. (2001). Multifocal ERG findings in complete type congenital stationary night blindness. *Investigative Ophthalmology & Visual Science, 42*, 1342–1348.

Kondo, M., Piao, C. H., Tanikawa, A., Horiguchi, M., Terasaki, H., & Miyake, Y. (2000). Amplitude decrease of photopic ERG b-wave at higher stimulus intensities in humans. *Japanese Journal of Ophthalmology, 44*, 20–28.

Leifert, D., Todorova, M. G., Prunte, C., & Palmowski-Wolfe, A. M. (2005). LED-generated multifocal ERG on- and off-responses in complete congenital stationary night blindness—A case report. *Documenta Ophthalmologica, 111*, 1–6.

Marmor, M. F., Hood, D. C., Keating, D., Kondo, M., Seeliger, M. W., & Miyake, Y. (2003). Guidelines for basic multifocal electroretinography (mfERG). *Documenta Ophthalmologica, 106*, 105–115.

Miyake, Y. (1988b). Studies of local macular ERG [in Japanese]. *Journal of Japanese Ophthalmological Society, 92*, 1418–1449.

Miyake, Y., Horiguchi, M., Suzuki, S., Kondo, M., & Tanikawa, A. (1997). Complete and incomplete type congenital stationary night blindness as a model of "OFF-retina" and "ON-retina". In M. M. LaVail, J. G. Hollyfield, & R. E. Anderson (Eds.), *Degenerative retinal diseases* (pp. 31–41). New York: Plenum Publishing.

Miyake, Y., Shiroyama, N., Ota, I., & Horiguchi, M. (1988a). Oscillatory potentials in electroretinograms of the human macular region. *Investigative Ophthalmology & Visual Science, 29*, 1631–1635.

Miyake, Y., Yagasaki, K., Horiguchi, M., & Kawase, Y. (1987). On- and off-responses in photopic electroretinogram in complete and incomplete types of congenital stationary night blindness. *Japanese Journal of Ophthalmology, 31*, 81–87.

Miyake, Y., Yagasaki, K., Horiguchi, M., Kawase, Y., & Kanda, T. (1986). Congenital stationary night blindness with negative electroretinogram: A new classification. *Archives of Ophthalmology, 104*, 1013–1020.

Pusch, C. M., Zeitz, C., Brandau, O., Pesch, K., Achatz, H., Feil, S., et al. (2000). The complete form of X-linked congenital stationary night blindness is caused by mutations in a gene encoding a leucine-rich repeat protein. *Nature Genetics, 26*, 324–327.

Rangaswamy, N. V., Hood, D. C., & Frishman, L. J. (2003). Regional variations in local contributions to the primate photopic flash ERG: Revealed using the slow-sequence mfERG. *Investigative Ophthalmology & Visual Science, 44*, 3233–3247.

Saeki, M., & Gouras, P. (1996). Cone ERGs to flash trains: The antagonism of a later flash. *Vision Research, 36*, 3229–3235.

Sieving, P. A., Murayama, K., & Naarendorp, F. (1994). Push-pull model of the primate photopic electroretinogram: a role for hyperpolarizing neurons in shaping the b-wave. *Visual Neuroscience, 11*, 519–532.

Terasaki, H., Miyake, Y., Nomura, R., Horiguchi, M., Suzuki, S., & Kondo, M. (1999). Blue-on-yellow perimetry in the complete type of congenital stationary night blindness. *Investigative Ophthalmology & Visual Science, 40*, 2761–2764.

Ueno, S., Kondo, M., Niwa, Y., Terasaki, H., & Miyake, Y. (2004). Luminance dependence of neural components that underlies the primate photopic electroretinogram. *Investigative Ophthalmology & Visual Science, 45*, 1033–1040.

Ueno, S., Kondo, M., Ueno, M., Miyata, K., Terasaki, H., & Miyake, Y. (2006). Contribution of retinal neurons to d-wave of primate photopic electroretinograms. *Vision Research, 46*, 658–664.

Young, R. S. L. (1991). Low-frequency component of the photopic ERG in patients with X-linked congenital stationary night blindness. *Clinical Vision Science, 6*, 309–315.

Young, R. S. L., Price, J., & Harrison, J. (1986). Psychophysical study of rod adaptation in patients with congenital stationary night blindness. *Clinical Vision Science, 1*, 137–143.

Recording Focal Macular Photopic Negative Response (PhNR) from Monkeys

Mineo Kondo, Yukihide Kurimoto, Takao Sakai, Toshiyuki Koyasu, Kentaro Miyata, Shinji Ueno, and Hiroko Terasaki

Purpose. To record the photopic negative response (PhNR) of the focal electroretinograms (ERGs) from the macula of monkeys and to study the properties of the focal macular PhNRs.

Methods. Focal macular ERGs were recorded from five rhesus monkeys using a modified infrared fundus camera, in which a red stimulus spot on a blue illuminated background were incorporated. The effects of different stimulus intensities and durations presented on a steady blue background of 100 scot cd/m^2 on the focal macular PhNRs were investigated. Focal macular PhNRs were also recorded before and after an intravitreous injection of tetrodotoxin (TTX).

Results. Focal ERG responses from a photocoagulated retinal site were recordable when the luminance of the red stimulus spot was ≤55 phot cd/m^2 and was presented on a steady blue background of 100 scot cd/m^2. The amplitude of the focal macular PhNR increased with increasing stimulus intensities and was larger than that of the b-wave at all stimulus intensities. The amplitude of the focal macular PhNR was largest at stimulus durations of 30 to 50 ms. An intravitreous injection of TTX essentially eliminated the focal macular PhNR.

Conclusions. It is possible to record focal macular PhNRs from monkeys by using a red stimulus spot on a blue background. Investigations of focal PhNRs can be a useful method of studying inner retinal function of local areas in normal and diseased retinas. (*Invest Ophthalmol Vis Sci.* 2008;49:3544–3550) DOI: 10.1167/iovs.08-1798

The photopic negative response (PhNR) is a slow, negative-going wave of the photopic electroretinogram (ERG) that appears immediately after the b-wave. This component was first identified by Viswanathan et al.[1] in 1999. They demonstrated that the PhNR was reduced in eyes of monkeys with increased intraocular pressure and reduced visual field sensitivity. In addition, they reported that the PhNR was essentially eliminated by an intravitreous injection of tetrodotoxin (TTX),[1–3] a selective blocker of voltage-gated Na^+ channels.[4–6] These results suggest that the PhNR originates mainly from the spiking activity of inner retinal neurons including the retinal ganglion cells and their axons.

In clinical studies, the PhNR has been reported to be reduced in patients with glaucoma,[7–9] optic nerve diseases,[10–12] and retinal vascular diseases that predominantly affect the inner retina.[13–15] We have reported that the amplitude of the PhNR is selectively reduced after macular hole surgery, indicating that there are some functional impairments in the inner retina after this type of surgery.[16] The results of these clinical studies suggest that recordings of the PhNR can provide a means for objective assessment of inner retinal function.

To date, the PhNR has been elicited mainly by full-field stimuli in both basic and clinical studies. However, the full-field ERG is the summed response from the entire retina, and it is difficult to assess the function of localized retinal areas by full-field ERGs. There are some reports on recording the PhNR from localized retinal areas,[2,7,17,18] but the characteristics of the focal PhNR in primates is less well understood. The focal PhNR is important because many diseases, including glaucoma and optic nerve diseases, affect selective areas of the retina. Therefore, we believed that developing a technique to record focal PhNRs could be useful for both basic research and clinical applications.

Thus, the purpose of this study was to determine whether a focal PhNR could be recorded from local areas of the monkey retina. For this, we developed a new recording system with a modified infrared fundus camera. A red stimulus spot was used on a blue illuminated background, because it has been reported recently that this color combination is most effective in eliciting large PhNRs especially at weak to moderate stimulus intensities.[3]

Methods

Stimulus and Observation Systems

Our new system for eliciting and recording focal PhNRs consisted of a modified infrared fundus camera and a stimulator that controlled the light-emitting diodes (LEDs) used for the stimulus and background illumination (Fig. 1A). An infrared television fundus camera (model VX-10; Kowa, Tokyo, Japan) was modified to obtain a Maxwellian stimulating system (Fig. 2). The image from this fundus camera was fed to a television monitor with a 45° view of the posterior pole of the eye (Fig. 1B). The position of the stimulus spot on the fundus was monitored on the television screen, and could be moved by the examiner with a joystick (Fig. 1A).

A red LED (λ_{max} = 627 nm; LXK2-PD12-S00; Philips Lumileds, San Jose, CA) was used as the stimulus source, and a blue LED (λ_{max} = 450 nm; L450, Epitex, Kyoto, Japan) was used for the background illumination that covered a retinal area of 45° (Fig. 2). The 15° red stimulus spot on the blue background that was photographed with a digital camera placed at the position of the monkey's eye is shown in Figure 1C. The size of the stimulus spot could be changed from 5° to 15°; the 15° stimulus spot was mainly used in this study.

The luminance of the blue background was fixed at 100 scot cd/m^2, which is known to be high enough to suppress the rod photoreceptors. The luminance of the red stimulus spot was increased from 2 to 204 phot cd/m^2, and the stimulus duration was increased from 5 to 150

From the Department of Ophthalmology, Nagoya University Graduate School of Medicine, Nagoya, Japan.

Supported by Health Sciences Research Grants (H16-sensory-001) from the Ministry of Health, Labor and Welfare, Japan, and by Grants 18591913 and 18390466 from the Ministry of Education, Culture, Sports, Science and Technology, Japan.

Submitted for publication January 27, 2008; revised March 29, 2008; accepted June 16, 2008.

Disclosure: **M. Kondo**, None; **Y. Kurimoto**, None; **T. Sakai**, None; **T. Koyasu**, None; **K. Miyata**, None; **S. Ueno**, None; **H. Terasaki**, None

The publication costs of this article were defrayed in part by page charge payment. This article must therefore be marked "*advertisement*" in accordance with 18 U.S.C. §1734 solely to indicate this fact.

Corresponding author: Mineo Kondo, Department of Ophthalmology, Nagoya University Graduate School of Medicine, 65 Tsuruma-cho, Showa-ku, Nagoya 466-8550, Japan; kondomi@med.nagoya-u.ac.jp.

Investigative Ophthalmology & Visual Science, August 2008, Vol. 49, No. 8

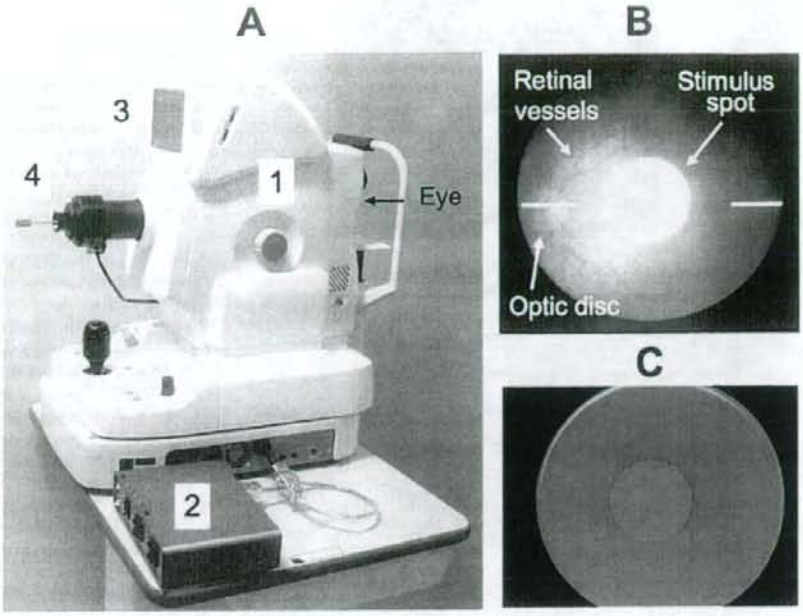

FIGURE 1. (**A**) Stimulus and observation system for recording the focal PhNR. This system consists of a modified infrared fundus camera (1) and LED control box (2). The infrared fundus image can be observed on a monitor (3), and the stimulus spot can be moved with a joystick (4). (**B**) Infrared fundus image of the monkey retina. A 15° stimulus spot positioned on the monkey's macula. (**C**) Image of the *red* stimulus spot on the *blue* background. This image was photographed by a digital camera at the position of the monkey's eye.

ms. The stimulus intensity was also expressed in energy units (i.e., phot cd-s/m^2, for brief flashes of ≤30 ms). The stimulus repetition rate was fixed at 2 Hz.

The luminances of the stimulus and background illumination were measured at the position of the corneal surface and then converted to the value at the retinal surface. These luminances were measured with a photometer (model IL 1700; International Light, Newburyport, MA).

Recording and Analyses

ERGs were recorded with a Burian-Allen bipolar contact lens electrode (Hansen Ophthalmic Development Laboratories, Iowa City, IA). The ground electrode was attached to the ipsilateral ear. The responses were amplified, and the band-pass filters were set at 0.5 to 1000 Hz. The ERGs were digitized at 5 kHz, and 100 to 300 responses were averaged for each recording (MEB-9100 Neuropack; Nihon Kohden, Tokyo, Japan).

The amplitude of the PhNR was measured from the baseline to the bottom of the negative trough after the b-wave for the brief flashes (≤ 30 ms), or was measured from the positive peak of the b-wave to the negative trough after the b-wave for the long-duration flashes (≥50 ms), as in previous studies.[1–5] The amplitudes of the a- and b-waves were measured from the baseline to the first negative trough and from the negative trough to the next positive peak, respectively.

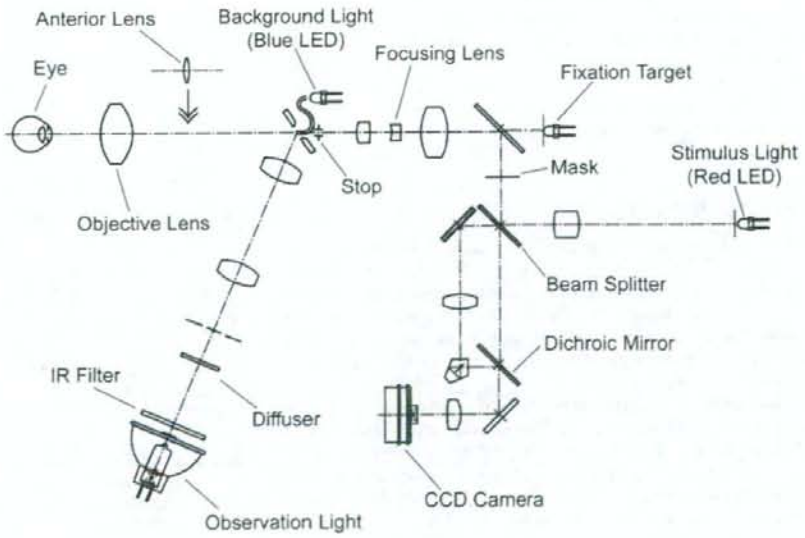

FIGURE 2. Diagram of the focal PhNR recording system with fundus monitoring with an infrared fundus camera. A red LED was used for the stimulus source, and a blue LED was used for the background illumination.

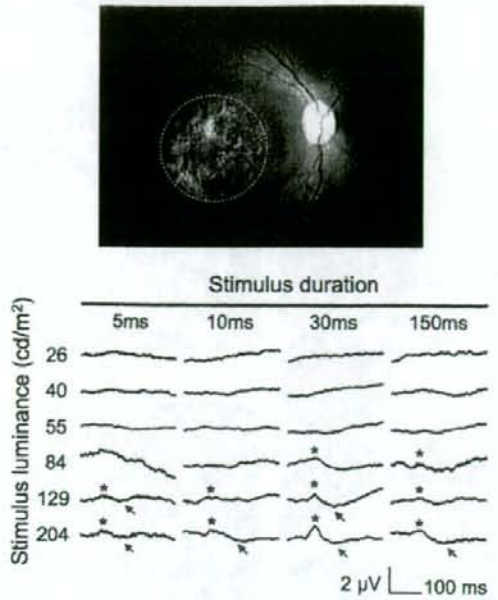

FIGURE 3. Studies of stray light effect in our system. (**A**) Fundus photograph of a monkey whose macula was damaged by 15° in the central area by focal laser photocoagulation (within the *white dashed line*). (**B**) Focal ERGs recorded with a 15° stimulus spot centered on the photocoagulation. Stimulus luminance and stimulus duration were changed on a steady blue background illumination of 100 scot cd/m². Small positive (*red asterisks*) or negative (*blue arrows*) waves were detected when the stimulus luminance was 84 cd/m² or higher, presumably due to the effect of stray light.

Animals

Five eyes of five rhesus monkeys (*Macaca mulatta*) were studied. The animals were sedated with an intramuscular injection of ketamine hydrochloride (7 mg/kg initial dose; 5 to 10 mg/kg/h maintenance dose) and xylazine (0.6 mg/kg). The respiration and heart rate were monitored, and hydration was maintained with slow infusion of lactated Ringer solution. The cornea was anesthetized with topical 1% tetracaine, and the pupils dilated with topical 0.5% tropicamide, 0.5% phenylephrine HCl, and 1% atropine. All experimental and animal care procedures adhered to the ARVO Statement for the Use of Animals in Ophthalmic and Vision Research and were approved by the Institutional Animal Care Committee of the Nagoya University.

Drug Application

The drugs and intravitreous injection techniques have been described in detail.[1-3,17,19,20] The drugs were injected into the vitreous with a 30-gauge needle inserted through the pars plana approximately 3 mm posterior to the limbus. TTX (Kanto Chemical, Tokyo Japan) was dissolved in sterile saline, and 0.05 to 0.07 mL was injected. The intravitreous concentration of TTX was 4 μM, assuming that the monkey's vitreous volume is 2.1 mL.

Because the TTX effect reaches its maximum at approximately 60 minutes after the drug injection, recordings were begun approximately 60 to 90 minutes after the injections, and studies were completed within 3 hours. Although the effects of these drugs are mostly reversible after a recovery period of several weeks, the results that are shown were recorded from eyes not previously treated.

RESULTS

Effects of Stray Light

To determine that the PhNRs we recorded were indeed focal responses, we investigated the effect of stray light on the responses with our system. First, we recorded focal ERGs using a 5° stimulus spot placed on the optic nerve head of monkeys. Different stimulus luminances (2–204 phot cd/m²) and stimulus durations (5, 10, 30, and 150 ms) were presented on a steady blue background illumination of 100 scot cd/m². There were no detectable ERG responses (<0.4 μV) when the stimulus luminance was ≤55 phot cd/m² for all stimulus durations. A small positive or negative response was elicited by a stimulus luminance of 84 phot cd/m² and stimulus durations of 30 and 150 ms. The amplitudes of the response increased with increasing stimulus luminance (data not shown).

We next examined the stray light effect by recording focal ERGs 1 month after an argon laser photocoagulation of a 15° spot in the macular area (Fig. 3A). ERGs were elicited by stimulating the photocoagulated area with different stimulus luminances (26–204 phot cd/m²), stimulus durations (5, 10, 30, and 150 ms), and a 15° stimulus spot. The stimulus spot was presented on a steady blue background illumination of 100 scot cd/m² in one monkey. We found that the response amplitudes were lower than the noise level (< 0.4 μV) when the stimulus luminance was ≤55 phot cd/m² for all stimulus durations. A small positive wave (Fig. 3B, red asterisks) or negative wave (blue arrows) was recorded when the stimulus luminance was ≥84 phot cd/m². These small responses were more prominent at stimulus durations of 30 and 150 ms and were most likely due to stray light, because the central retina within 15° had been completely photocoagulated.

Based on these results, we concluded that stimulus luminances of ≤55 phot cd/m² presented on a steady blue background of 100 scot cd/m² are the optimal stimulus for eliciting focal ERGs in our system.

Effect of Stimulus Intensity

Representative focal macular ERGs elicited by stimulus luminances of 2 to 55 phot cd/m² for four stimulus durations of 5, 10, 30, and 150 ms are shown in Figure 4. It is clear that the amplitude of the focal PhNRs increased with increasing stimulus luminance for all stimulus durations.

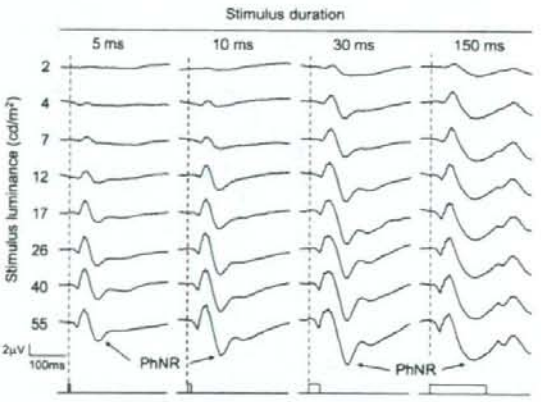

FIGURE 4. Representative focal ERGs elicited from a rhesus monkey by different stimulus luminances (2–55 phot cd/m²) and different stimulus durations (5, 10, 30, and 150 ms). The amplitude of PhNR increases with increasing stimulus luminances.

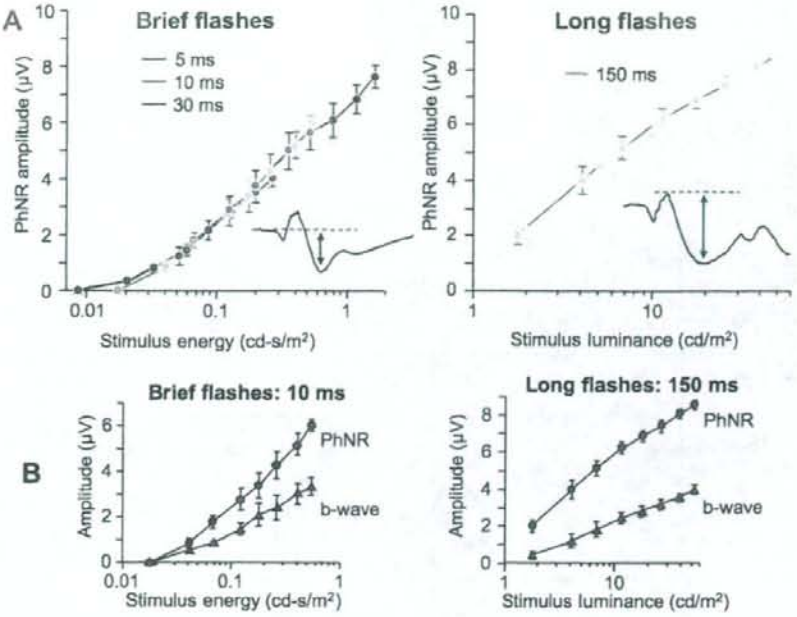

FIGURE 5. (A) Stimulus intensity–response curves of the mean (± SEM, $n = 4$) amplitudes of the focal macular PhNR. The PhNR amplitudes are plotted as a function of stimulus energy (cd-s/m^2) for brief flashes of 5 to 30 ms in the left half and are plotted as a function of stimulus luminance (cd/m^2) for a long 150-ms flash in the right half. (B) Comparison of stimulus intensity–response curves of the mean (± SEM, $n = 4$) amplitudes of the b-wave and PhNR for stimulus duration of 10 ms (*left*) and 150 ms (*right*).

The relationship between the stimulus intensities and the average amplitudes of the focal macular PhNRs is shown in Figure 5A. The amplitudes of the focal macular PhNR are plotted as a function of stimulus energy for brief flashes (5, 10, and 30 ms, left), and are plotted as a function of stimulus luminance for long flashes (150 ms, right). We found that when the stimulus duration was shorter than the integration time of PhNR (≤ 30 ms), the amplitude of the focal macular ERG was dependent on the stimulus energy (Fig. 5A).

One of the interesting findings was that the amplitude of PhNR was larger than that of the b-wave for all stimulus intensities and was more than double the b-wave amplitude at a stimulus duration of 150 ms at all stimulus luminances (Fig. 5B).

Effect of Stimulus Duration

We also examined the effects of stimulus duration on the focal macular PhNR of monkeys. Representative focal macular ERGs elicited by different stimulus durations of 5 to 150 ms at a constant stimulus luminance of 55 phot cd/m^2 are shown in Figure 6A. The stimulus energy (phot cd-s/m^2) is also indicated for the brief flashes of ≤30 ms.

The amplitude of the focal macular PhNR increased with increasing stimulus durations when the stimulus durations were shorter than 30 to 50 ms. This increase in the amplitude is most likely due to the increase in the stimulus energy (see also Fig. 5A). Further increases in the stimulus duration led to a slight decrease in the PhNR amplitude (Fig. 6B).

We also found that the implicit time of the PhNR was dependent on the stimulus duration. The implicit time of the PhNR was approximately 75 ms for a stimulus of 5 ms duration and became longer with increasing stimulus durations and then reached a maximum implicit time (110 ms) at approximately 50 ms duration (Fig. 6A, red dashed vertical lines). This gradual increase in the implicit time of the PhNR most likely resulted from an increase in stimulus energy and the increase in the midpoint of the stimulus. Further increases in the stimulus duration did not change the implicit time of the PhNR.

We also found that another slow negative response (Fig. 6A, asterisks) developed after the stimulus offset for longer stimulus durations of 100 to 150 ms. This negative response was thought to be a homologue of the PhNR to the stimulus offset ($PhNR_{Off}$), which has been reported in studies of full-field photopic ERGs.[1–3,20]

Effect of Intravitreous Injection of TTX

Finally, we studied whether the focal macular PhNR recorded from monkeys changed after an intravitreous injection of TTX, which blocks voltage-gated sodium channels and prevents the generation of sodium-based action potentials. Representative waveforms of focal macular ERGs recorded before (black) and after (red) an intravitreous injection of TTX are shown in Figure 7. The stimulus luminance was set at 55 phot cd/m^2, and the responses to stimulus durations of 5 to 150 ms are shown. We found that blocking the spiking activities of inner retinal neurons by TTX essentially eliminated the focal macular PhNR, which was similar to the effect of TTX on the full-field photopic ERG.[1–3]

For long-duration stimuli of 100 to 150 ms, the slow negative potential that was found after the light offset ($PhNR_{Off}$, Fig. 7, asterisks) was also not present after TTX. Similar effects have been reported for full-field ERG studies.[1–3,20]

Although the major effect of TTX was seen in the PhNR, other ERG components of the focal macular ERG were also slightly altered after TTX. The amplitude of the a-wave became slightly smaller, and the implicit times of the b-wave were delayed. These minor changes were also very similar to those reported for full-field PhNR studies.[1–3]

Discussion

Our results showed that focal PhNRs can be recorded from the macular area of monkeys by using our newly developed system. In this system, a red stimulus spot was presented on a blue background, which was earlier shown to be the optimal stim-

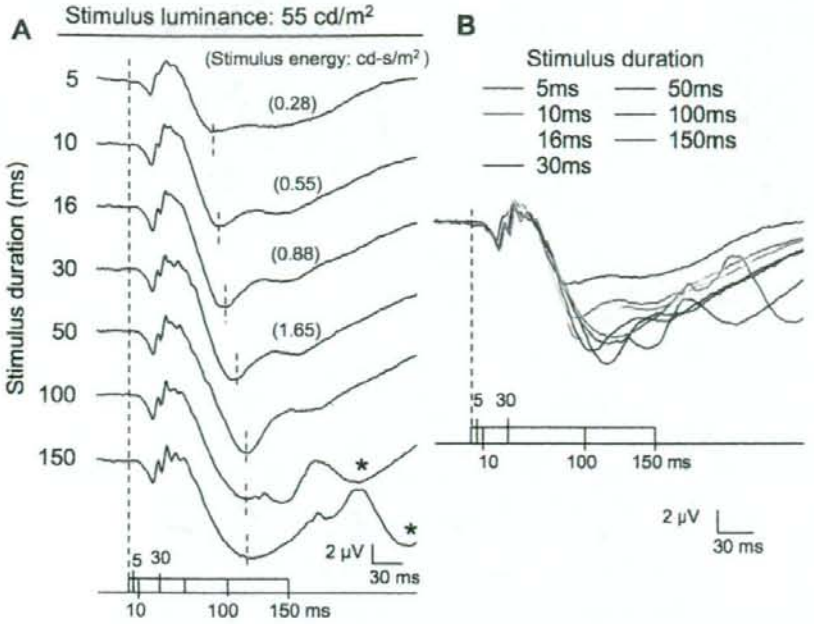

FIGURE 6. Effect of stimulus duration on the focal PhNR. (**A**) Representative focal ERGs elicited by different stimulus durations (5–150 ms) for a constant stimulus luminance of 55 phot cd/m². *Vertical dotted line*: peak of the PhNR. The values of stimulus energy (cd-s/m²) are also indicated for brief flashes of 5 to 30 ms. (**B**) Superimposed focal ERG waveforms recorded with different stimulus durations (5–150 ms). Stimulus luminance was fixed at 55 phot cd/m².

ulus conditions to elicit large PhNRs especially at low to intermediate stimulus intensities.[3] In addition, our system allowed us to monitor the position of the stimulus spot on the monkey's fundus during the recordings. Our ability to record focal PhNRs from monkey eyes is important, because this will allow us to manipulate the recording conditions or alter the normal PhNR with drugs known to affect specific neural elements to study the physiological properties of the PhNRs.

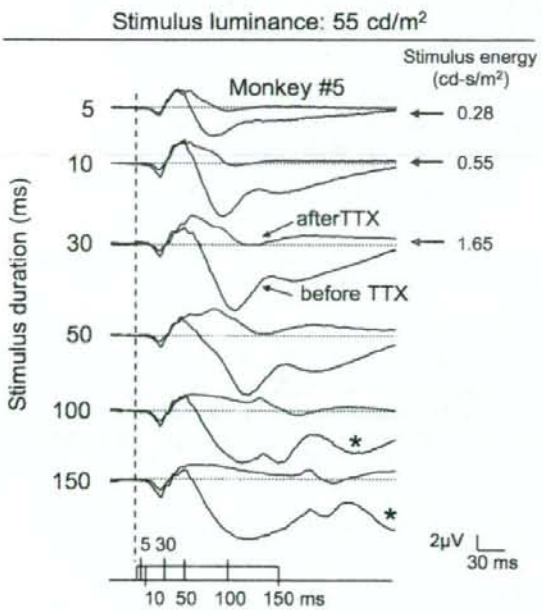

FIGURE 7. Focal ERGs before and after intravitreous injection of TTX in one monkey. The focal ERGs before (*black lines*) and after TTX (*red lines*) are superimposed. Stimulus luminance was fixed at 55 phot cd/m², and stimulus duration was changed from 5 to 150 ms. Note that the amplitude of focal PhNR was greatly reduced after TTX. The other slow negative response to the stimulus offset ($PhNR_{Off}$, asterisks) was also reduced after TTX.

To establish a technique to record focal ERGs, it was important for us to determine the optimal combination of stimulus and background intensities.[21–28] Based on the results of trying to elicit focal ERGs from the optic nerve head and from a retinal site damaged by focal laser coagulation, we found that a 15° red stimulus spot of ≤55 phot cd/m² presented on a steady blue background of 100 scot cd/m², will elicit a focal ERG. For stimulus intensities >55 phot cd/m², small responses were recorded even from the retinal site damaged by focal laser coagulation, and this response was most likely due to stray light (Fig. 3). The stray light effect was dependent on the stimulus intensity and was greater for longer stimulus durations of 30 and 150 ms (Fig. 3B).

We studied the response characteristics of the focal macular PhNRs recorded by our system, and found the following: (1) The focal macular PhNR was a slow, negative response, with an implicit time of approximately 75 ms for short-duration stimuli and approximately 110 ms for long-duration stimuli (Fig. 6); (2) for long-duration stimuli, the PhNR was seen after both the onset and the offset of the stimulus (Figs. 4, 6); (3) the amplitude of the focal macular PhNR increased with increasing stimulus intensity (Fig. 5); and, (4) the amplitude of the focal macular PhNR was greatly reduced after an intravitreous injection of TTX.

These results showed that the response characteristics of focal PhNRs recorded from the monkey's macula were very similar to those of the full-field PhNR,[1–3,11] and that this negative response originates mainly from the action potentials of the inner retinal neurons.

One interesting finding in our study was that the amplitudes of focal macular PhNRs recorded by our system were large; the maximum PhNR amplitude reached 6.1 μV for a 10-ms

duration stimulus and 8.3 μV for a 150-ms duration stimulus. The amplitudes of the focal PhNR recorded from the 15° macular area were relatively large when compared with the amplitudes of the full-field PhNR which were 25 to 40 μV in earlier monkey studies.[1-3,11] Large PhNR amplitudes in our focal ERGs can also be understood when one examines the amplitude of the b-wave and PhNR. The amplitude of PhNR was larger than that of the b-wave in all stimulus conditions and was more than twice that of the b-wave for long-duration stimuli of 150 ms (Fig. 5B).

The reason for the relatively large PhNR amplitude in the macular region in monkeys was not examined, but may be explained by two possibilities. First, the density of ganglion cells (number/mm^2) is highest in the central retina of monkeys,[29-33] and the slope of ganglion cell number as a function of retinal eccentricity is steeper than that of cone cells in the human retina.[34] This high ganglion cell density in the central retina may contribute to the large amplitude of the macular PhNR. And second, we used a red stimulus spot on a blue background. This combination was recently shown to be optimal for eliciting maximum PhNR amplitude. Using various stimulus and background color combinations, Rangaswamy et al.[3] concluded that at weak to moderate stimulus intensities, the amplitude of PhNR is larger in response to stimuli that are relatively more cone specific.

The amplitude of macular PhNR increased with increasing stimulus durations up to 30 to 50 ms, because of due to the increase in the stimulus energy. However, further increases in the stimulus duration led to a decrease in amplitude. The decrease in amplitude may be explained by the separation of the two PhNR components: $PhNR_{on}$ elicited by stimulus onset and $PhNR_{off}$ elicited by stimulus offset, both of which are superimposed when a brief-flash stimuli (≤50 ms) is used. A second possibility is that this amplitude decrease may be due to factors other than the spiking activities of inner retinal neurons. As seen in Figure 7, the longer duration stimuli tended to elicit prolonged b-waves (plateau) when the PhNR was eliminated by TTX, whereas the brief-flash responses generally leveled off at the baseline.

There remain some critical matters that should be addressed in future studies. First, we did not show how full-field PhNR and focal macular PhNR are different with regard to the intensity-response function, duration-response function, and the effect of TTX. To determine these differences, we must compare the full-field and focal PhNRs in the same stimulus and recording conditions. Second, although we succeeded in recording focal PhNRs from the macula of monkeys, we did not examine whether there are any regional variations across the retina in the waveform or amplitude of the PhNR. We are currently comparing the focal PhNRs between upper and lower retinas, or nasal and temporal retinas by using semicircular stimulus spots. Finally, in this study we used only one type of electrode, the Burian-Allen bipolar contact lens electrode. However, it is known that the speculum of this electrode, which also acts as the reference, can pick up signals that can cancel out the signals picked up by the corneal electrode. It may be better to place the reference farther from the recording electrode (e.g., fellow eye), to maximize the response of small signals.[35,36]

In conclusion, we successfully recorded focal PhNRs from the macula of monkeys by using a red stimulus spot on a blue background. Although there are still many factors that need to be tested, we believe that examinations of the focal PhNRs can be a useful technique for studying the inner retinal function of local retinal areas in normal and diseased retinas.

Acknowledgments

The authors thank Yozo Miyake of Shukutoku University and Duco I. Hamasaki for discussions on the manuscript, and Masao Yoshikawa, Hideteka Kudo, and Ei-ichiro Nagasaka of Mayo Corporation for technical assistance.

References

1. Viswanathan S, Frishman LJ, Robson JG, et al. The photopic negative response of the macaque electroretinogram: reduction by experimental glaucoma. *Invest Ophthalmol Vis Sci.* 1999;40:1124-1136.
2. Viswanathan S, Frishman LJ, Robson JG. The uniform field and pattern ERG in macaques with experimental glaucoma: removal of spiking activity. *Invest Ophthalmol Vis Sci.* 2000;41:2797-2810.
3. Rangaswamy NV, Shirato S, Kaneko M, et al. Effects of spectral characteristics of Ganzfeld stimuli on the photopic negative response (PhNR) of the ERG. *Invest Ophthalmol Vis Sci.* 2007;48:4818-4828.
4. Narahashi T, Moore JW, Scott WR. Tetrodotoxin blockage of sodium conductance increase in lobster giant axons. *J Gen Physiol.* 1964;47:965-974.
5. Bloomfield SA. Effect of spike blockade on the receptive-field size of amacrine and ganglion cells in the rabbit retina. *J Neurophysiol.* 1996;75:1878-1893.
6. Stafford DK, Dacey DM. Physiology of the A1 amacrine: a spiking, axon-bearing interneuron of the macaque monkey retina. *Vis Neurosci.* 1997;14:507-522.
7. Colotto A, Falsini B, Salgarello T, et al. Photopic negative response of the human ERG: Losses associated with glaucomatous damage. *Invest Ophthalmol Vis Sci.* 2000;41:2205-2211.
8. Viswanathan S, Frishman LJ, Robson JG, et al. The photopic negative response of the flash electroretinogram in primary open angle glaucoma. *Invest Ophthalmol Vis Sci.* 2001;42:514-522.
9. Drasdo N, Aldebasi YH, Chiti Z, et al. The S-cone PhNR and pattern ERG in primary open angle glaucoma. *Invest Ophthalmol Vis Sci.* 2001;42:1266-1272.
10. Gotoh Y, Machida S, Tazawa Y. Selective loss of the photopic negative response in patients with optic nerve atrophy. *Arch Ophthalmol.* 2004;122:341-346.
11. Rangaswamy NV, Frishman LJ, Dorotheo EU, et al. Photopic ERGs in patients with optic neuropathies: comparison with primate ERGs after pharmacologic blockade of inner retina. *Invest Ophthalmol Vis Sci.* 2004;45:3827-3837.
12. Miyata K, Nakamura M, Kondo M, et al. Reduction of oscillatory potentials and photopic negative response in patients with autosomal dominant optic atrophy with OPA1 mutations. *Invest Ophthalmol Vis Sci.* 2007;48:820-824.
13. Machida S, Gotoh Y, Tanaka M, Tazawa Y. Predominant loss of the photopic negative response in central retinal artery occlusion. *Am J Ophthalmol.* 2004;137:938-940.
14. Kizawa J, Machida S, Kobayashi T, et al. Changes of oscillatory potentials and photopic negative response in patients with early diabetic retinopathy. *Jpn J Ophthalmol.* 2006;50:367-373.
15. Chen H, Wu D, Huang S, Yan H. The photopic negative response of the flash electroretinogram in retinal vein occlusion. *Doc Ophthalmol.* 2006;113:53-59.
16. Ueno S, Kondo M, Piao CH, et al. Selective amplitude reduction of the PhNR after macular hole surgery: ganglion cell damage related to ICG-assisted ILM peeling and gas tamponade. *Invest Ophthalmol Vis Sci.* 2006;47:3545-3549.
17. Rangaswamy NV, Hood DC, Frishman LJ. Regional variations in local contributions to the primate photopic flash ERG: revealed using the slow-sequence mfERG. *Invest Ophthalmol Vis Sci.* 2003;44:3233-3247.
18. Fortune B, Wang L, Bui BV, et al. Local ganglion cell contributions to the macaque electroretinogram revealed by experimental nerve fiber layer bundle defect. *Invest Ophthalmol Vis Sci.* 2003;44:4567-4579.
19. Ueno S, Kondo M, Niwa Y, et al. Luminance dependence of neural components that underlies the primate photopic electroretinogram. *Invest Ophthalmol Vis Sci.* 2004;45:1033-1040.

20. Ueno S, Kondo M, Ueno M, et al. Contribution of retinal neurons to d-wave of primate photopic electroretinograms. *Vision Res*. 2006;46:658–664.
21. Brindley GS, Westheimer G. The spatial properties of the human electroretinogram. *J Physiol*. 1965;179:518–537.
22. Aiba TS, Alpern M, Maaseidvaag F. The electroretinogram evoked by the excitation of human foveal cones. *J Physiol*. 1967;189:43–62.
23. Jacobson JH, Kawasaki K, Hirose T. The human electroretinogram and occipital potential in response to focal illumination of the retina. *Invest Ophthalmol*. 1969;8:545–556.
24. Biersdorf WR, Diller DA. Local electroretinogram in macular degeneration. *Am J Ophthalmol*. 1969;68:296–303.
25. Hirose T, Miyake Y, Hara A. Simultaneous recording of electroretinogram and visual evoked response: focal stimulation under direct observation. *Arch Ophthalmol*. 1977;95:1205–1208.
26. Sandberg MA, Ariel M. A hand-held, two-channel stimulator-ophthalmoscope. *Arch Ophthalmol*. 1977;95:1881–1882.
27. Seiple WH, Siegel IM, Carr RE, Mayron C. Evaluating macular function using the focal ERG. *Invest Ophthalmol Vis Sci*. 1986;27:1123–1130.
28. Miyake Y, Shiroyama N, Horiguchi M, Ota I. Asymmetry of focal ERG in human macular region. *Invest Ophthalmol Vis Sci*. 1989;30:1743–1749.
29. Rolls ET, Cowey A. Topography of the retina and striate cortex and its relationship to visual acuity in rhesus monkeys and squirrel monkeys. *Exp Brain Res*. 1970;10:298–310.
30. Webb SV, Kaas JH. The sizes and distribution of ganglion cells in the retina of the owl monkey Aotus trivirgatus. *Vision Res*. 1976;16:1247–1254.
31. DeBruyn EJ, Wise VL, Casagrande VA. The size and topographic arrangement of retinal ganglion cells in the galago. *Vision Res*. 1980;20:315–327.
32. Stone J, Johnston E. The topography of primate retina: a study of the human, bushbaby, and new- and old-world monkeys. *J Comp Neurol*. 1981;196:205–224.
33. Perry VH, Cowey A. The ganglion cell and cone distributions in the monkey's retina: implications for central magnification factors. *Vision Res*. 1985;25:1795–1810.
34. Curcio CA, Allen KA. Topography of ganglion cells in human retina. *J Comp Neurol*. 1990;300:5–25.
35. Sutter EE, Bearse MA Jr. The optic nerve head component of the human ERG. *Vision Res*. 1999;39:419–436.
36. Hood DC, Bearse MA Jr, Sutter EE, et al. The optic nerve head component of the monkey's (Macaca mulatta) multifocal electroretinogram (mERG). *Vision Res*. 2001;41:2029–2041.

Correlation between Macular Volume and Focal Macular Electroretinogram in Patients with Retinitis Pigmentosa

Tadasu Sugita, Mineo Kondo, Chang-Hua Piao, Yasuki Ito, and Hiroko Terasaki

Purpose. To determine whether a significant correlation exists between the morphology of the macula measured by optical coherence tomography (OCT) and the amplitude of focal macular electroretinograms (fmERGs) in patients with retinitis pigmentosa (RP).

Methods. fmERGs were recorded in 43 patients with RP and 43 age-similar normal subjects, with a 15° stimulus spot, 5.6 to 5.8 mm in diameter on the fundus. The sum of the volume of the neural retina in the central 6 mm (total macular volume) was measured with the OCT system. The length of the photoreceptor inner segment/outer segment junction (IS/OS line) in a 6-mm diameter macular area was also measured in the OCT images.

Results. There was a weak correlation between the total macular volume and the fmERG amplitudes (correlation coefficient, 0.46 for the a-wave and 0.54 for the b-wave). The fmERG amplitudes in the patients with RP with IS/OS line longer than 2 mm were significantly larger than those in patients with RP with IS/OS line shorter than 2 mm, but the correlations between these two factors were weak. One major reason for the low correlations between the macular morphology and fmERGs was that there were some patients with RP who had normal macular volume and long IS/OS line, but had severely reduced focal macular ERGs.

Conclusions. Although the macular volume and length of the IS/OS line correlated weakly with the amplitude of the fmERGs, a preserved macular morphology does not necessarily guarantee normal-amplitude fmERGs in patients with RP. (*Invest Ophthalmol Vis Sci.* 2008;49:3551–3558) DOI:10.1167/iovs.08-1954

Retinitis pigmentosa (RP) is a subset of inherited retinal diseases characterized by a progressive loss of the rod and cone photoreceptors.[1–5] Past histopathologic studies on patients with RP[6–8] have shown that the earliest anatomic change is a shortening or distortion of the rod and cone photoreceptor outer segments. This change is followed by the loss of rod and cone photoreceptors beginning in the periphery and progressing toward the central retina.

It is important to evaluate the functional and structural changes in the macular area of patients with RP because the central retina is relatively better preserved until the late stages, and various subjective and objective examinations have been used. Focal ERGs[9–13] and multifocal ERGs[14–21] have been used to assess the macular function of eyes with RP, because these techniques can examine the neural activities of the macular area objectively.

Optical coherence tomography (OCT) is a noninvasive technique that can assess the morphology of the retina, especially the macula in vivo. This technique is especially useful in patients with RP, because OCT enables the investigator to evaluate the morphologic changes in each retinal layer and the overall retina.[22–26] It has been shown that the OCT-determined cross-sectional retinal images were well-correlated with retinal histology in animal models of retinal degeneration.[27–40] In addition, there is evidence that the OCT-determined structural changes in the central retina correlate with subjective visual functions including the visual acuity and visual threshold in patients with RP.[27,30,34,36] However, there is only one report on the relationship between the morphologic changes measured by OCT and macular function measured by focal macular ERGs (fmERGs) in patients with RP.[25] The relationship between the macular morphology and function in patients with RP can provide important information on the treatment of patients with retinal degeneration.[29,31–33]

Thus, the purpose of this study was to determine whether a significant correlation exists between the amplitude of the fmERGs and the sum of the volume of the neural retina in the central 6 mm of the macula (total macular volume) or the length of the photoreceptor inner/outer segment junction (IS/OS line) measured by OCT images in patients with typical retinitis pigmentosa (RP).

Methods

Subjects

This prospective study included 124 consecutive patients with RP who visited one ophthalmologist (MK) in the Department of Ophthalmology, Nagoya University Hospital, from January to December in 2006. The clinical diagnosis of RP was based on the ocular history, funduscopic findings, visual fields, and ISCEV (International Society for Clinical Electrophysiology of Vision) standard full-field ERGs.[41] The inclusion criteria were a diagnosis of RP with a complete medical examination, including best corrected visual acuity (BCVA) measured by the standard Japanese decimal visual acuity chart, fundus examination, Goldmann kinetic visual fields, full-field ERGs; BCVA had to be ≥0.3. The exclusion criteria were atypical RP (e.g., central RP, sector RP, or unilateral RP), opacities in the media including cataracts, and cystoid macular edema identified by the OCT. Based on these inclusion and exclusion criteria, 43 eyes of 43 patients with RP (19 males, 24 females; mean age, 41.7 years; range, 16–66) were analyzed. If both eyes met these criteria, then the data from only the right eye were used for the analyses.

The inheritance pattern was autosomal dominant in 6 (14%) patients, autosomal recessive in 6 (14%), and sporadic in 31 (72%). None of the patients was found to have X-linked RP. The best corrected visual acuity ranged from 0.3 to 1.2, and the mean logarithm of the minimum angle of resolution (logMAR) was 0.052 units.

For controls, fmERGs and OCT were recorded from 43 age-similar normal subjects (14 males, 29 females; mean age, 42.7 years, range,

From the Department of Ophthalmology, Nagoya University Graduate School of Medicine, Nagoya, Japan.

Supported by Grants-in Aid 18591913 (MK), 19500416 (YI), and 18390466 (HT) from the Ministry of Education, Culture, Sports, Science and Technology.

Submitted for publication February 29, 2008; revised April 13, 2008; accepted June 16, 2008.

Disclosure: **T. Sugita**, None; **M. Kondo**, None; **C.-H. Piao**, None, **Y. Ito**, None; **H. Terasaki**, None

The publication costs of this article were defrayed in part by page charge payment. This article must therefore be marked "*advertisement*" in accordance with 18 U.S.C. §1734 solely to indicate this fact.

Corresponding author: Mineo Kondo, Department of Ophthalmology, Nagoya University Graduate School of Medicine, 65 Tsuruma-cho, Showa-ku, Nagoya 466-8550, Japan; kondomi@med.nagoya-u.ac.jp.

16–67). None had known abnormalities of the visual system, and their visual acuity was ≥1.0 in all.

The research was conducted in accordance with the Institutional Guidelines of Nagoya University and conformed to the tenets of the World Medical Association's Declaration of Helsinki. Informed consent was obtained from each of the patients after they were provided sufficient information on the procedures to be used.

Focal Macular ERGs

The stimulus and recording systems used to record fmERGs have been described in detail.[15,42,43] Briefly, an infrared fundus camera equipped with a stimulus light, background illumination, and fixation target was used. The image from the camera was fed to a television monitor, and the examiner used the image on the monitor to maintain the stimulus on the macula. A stimulus spot size of 15° was selected because ocular biometry[44–46] has shown that a 15° stimulus spot covers a retinal area of 5.5 to 5.8 mm, which is approximately the size of the OCT-determined macular diameter (6.0 mm). The background light subtended a visual angle of 45°, and additional background illumination outside the central 45° produced a homogeneous background for nearly the entire visual field. The luminances of the white stimulus light and background light were 29.46 and 2.89 cd/m^2, respectively. Although this luminance of background light was not strong enough to suppress all the rod activity, we have shown that the fmERGs elicited by this method are generated mainly by the cone system, and the responses elicited by spot stimuli of 5 to 15° are local responses.[42,43]

A Burian-Allen bipolar contact lens electrode was used to record the fmERGs. This contact lens electrode system had low electrical noise and permitted a clear view of the fundus by the camera during the recordings. After the pupils were fully dilated with 0.5% tropicamide and 0.5% phenylephrine hydrochloride, fmERGs were elicited by a flicker train consisting of a square waves presented at 5 Hz (100-ms on and 100-ms off). Then, a series of 512 responses were averaged in a single cycle by a signal processor. The time constant of the bioamplifier was set at 0.03 seconds with a 100-Hz high-cut filter to record the a- and b-waves.

The amplitude of the a-wave was measured from the baseline to the first negative trough, and the amplitude of b-wave was measured from the trough of the a-wave to the positive peak of the b-wave.

OCT Measurements

The morphology of the macula was evaluated by a high-resolution optical coherence tomograph (Stratus model 3000, software ver. 4.0.1; Carl Zeiss Meditec, AG, Oberkochen, Germany). After the patients' pupils were fully dilated with 0.5% tropicamide and 0.5% phenylephrine, the sum of the volume of the neural retina in the central 6 mm of the macula (total macular volume) was measured using six scans of 6 mm in a radial pattern intersecting at the fixation point.

It is known that the automatic fast macular thickness map (FMTM) protocol often fails to identify the outer borders of the neural retina, which can lead to recording of erroneous retinal thicknesses and volumes.[47] Therefore, we used a program developed in our laboratory (Ishikawa K, et al. *IOVS* 2005;46:ARVO E-Abstract 1550),[48] by which the total macular volume was measured more precisely than that calculated by the conventional FMTM system. In this program, the user was able to set 20 cursors above and below a selected area manually. The inner cursors were set on the internal limiting membrane (ILM), and the outer cursors were set on the retinal pigment epithelium (RPE)–choriocapillaris hyperreflective complex borderline. Another set of cursors was set on the fovea of the OCT images. Then, each OCT radial scan was analyzed as a retinal map, and the total macular volume was calculated precisely by our software.

Past studies with the Stratus OCT and ultrahigh-resolution OCT demonstrated that there are two well-defined, parallel, highly reflective lines (HRLs) in the outer retinal layer.[49,50] It has been shown that the inner HRL corresponds to the photoreceptor inner/outer segment junction or the IS/OS line, and the outer HRL corresponds to the retinal pigment epithelium and choriocapillaris complex. To asses the relationship between the morphologic changes in the photoreceptor layer and the amplitude of the fmERGs, we classified the IS/OS line in patients with RP into three types: type 1, distinct IS/OS line longer than the central 2 mm; type 2, distinct IS/OS line only within the central 2 mm; and type 3, absence of IS/OS line within the central 6 mm (Fig. 1). To perform this classification, we reviewed the six tomographic images of each eye on a gray scale with an alignment image protocol, because the IS/OS line is more clearly visible on gray-scale tomographic images.[51] The classification was performed by TS in a masked manner.

Statistical Analyses

The significance of the differences between the patients with RP and normal control subjects was determined by nonparametric Mann-Whitney U tests. The correlations between the macular volume and the fmERG amplitudes were determined by the Spearman's rank correlation. Differences in the amplitudes among the three groups (types 1, 2, and 3) based on the length of the IS/OS line were analyzed with the nonparametric Kruskal-Wallis test and Scheffé's test, as the multiple comparison procedures. Differences and correlations were considered to be significant when $P < 0.05$.

Results

Representative OCT images and fmERGs recorded from one normal subject and three patients with RP are shown in Figure 2. The amplitudes of the fmERGs in case 1 were relatively well preserved, and the macular volume was within the normal range. The amplitudes of the fmERGs in case 2 were reduced, and the macular volume was close to the lower borderline of normal. The fmERGs in case 3 were nonrecordable, and the macular volume was severely reduced.

Box plots of the fmERG amplitudes (a- and b-waves) and total macular volume for 43 normal control subjects and 43 patients with RP are shown in Figure 3. As expected, both the amplitudes of the a- and b-waves of the fmERGs and the total

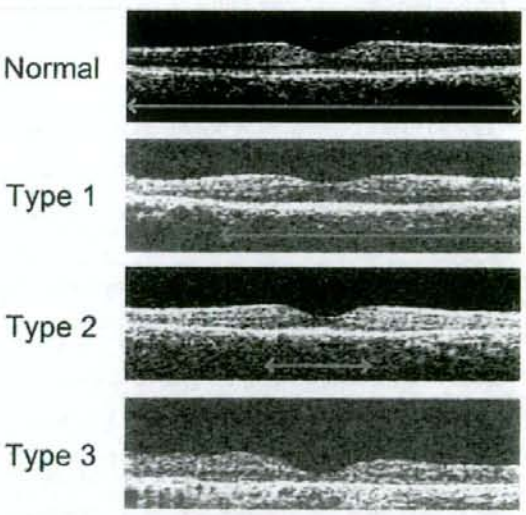

FIGURE 1. The photoreceptor IS/OS junction line in the OCT image can be divided into three categories; type 1, distinct IS/OS line over central 2 mm; type 2, distinct IS/OS line only within central 2 mm; type 3, absent IS/OS line. *Red lines*: the length of the IS/OS line, which was detected on the gray-scale OCT image.

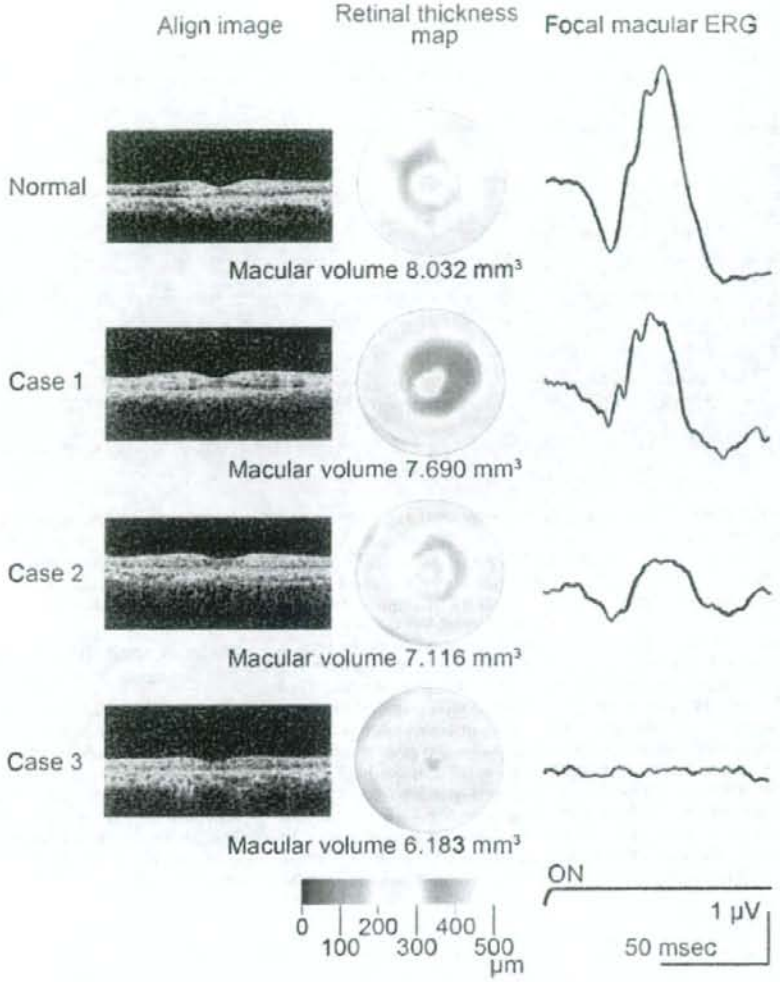

FIGURE 2. OCT images and fmERGs recorded from a normal subject and three representative patients with RP.

macular volume in patients with RP were significantly smaller than those of normal subjects ($P < 0.001$).

Correlation between Amplitude of fmERG and Macular Volume

Because changes in the macular morphology should lead to functional changes,[5,2] we investigated whether there was a correlation between the amplitude of fmERGs and the total macular volume in our 43 patients with RP. The amplitudes of the a- and b-waves for 43 patients with RP are plotted against the total macular volume in Figures 4A and 4B, respectively. For both graphs, the gray area shows the 2.5 to 97.5 percentiles of normal control subjects.

A significant but weak correlation was found between the fmERG amplitude and total macular volume (a-wave, $\rho = 0.458$, $P < 0.01$; b-wave, $\rho = 0.540$, $P < 0.01$; Spearman's rank correlation). One of the reasons for this relatively weak correlation between the fmERG amplitude and total macular volume was that there were four patients with RP who had normal macular volume but severely reduced fmERG (e.g., patients 4–7, Fig. 4). In contrast, there were no patients with RP who had normal a- and b-wave amplitudes with severely reduced macular volume. There were two patients with RP who had normal a-wave amplitude with reduced macular volume, but their macular volumes were still near the lower borderline of normal, and their b-wave amplitudes were lower than the normal range.

Correlation between fmERG and Length of IS/OS Line

We attempted to measure the thickness of each retinal layer (i.e., outer, middle, and inner retinal layers) separately, but found that it was very difficult to identify the border between these layers, especially in patients with relatively advanced stages of RP. The total macular volume is the sum of the volume of the neural retina in the central 6 mm of the retina and was used in the analyses. In addition, we used the length of the photoreceptor inner segment/outer segment junction

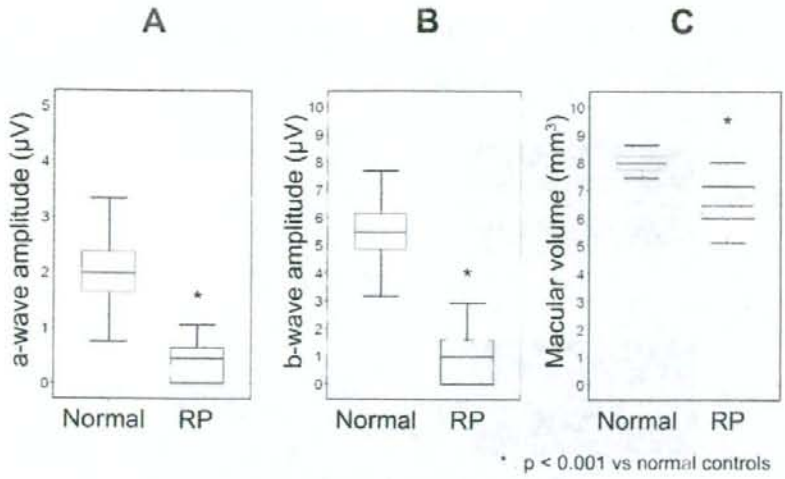

FIGURE 3. Box plots of the a- and b-waves of the fmERGs and total macular volume for normal controls and patients with RP. Line within the box indicates the median, the box the 25 and 75 percentiles, and the end of the error bars the 2.5 and 97.5 percentiles.

(IS/OS line) as a measure of the structural integrity of the macular area.

The amplitudes of the fmERG for the three RP groups classified by the length of the IS/OS line are shown in the upper traces of Figure 5 (see also Fig. 1). The amplitudes of the fmERGs in type 1 patients with RP (distinct IS/OS line over the central 2 mm) were significantly larger than those in type 2 (distinct IS/OS line only in the central 2 mm) and type 1 (absent IS/OS line) patients with RP ($P < 0.05$). Nine (81%) of 11 patients with type 3 RP had nonrecordable fmERGs, whereas none with type 1 had nonrecordable fmERGs (Fig. 5, bottom plot). These findings suggest that the patients with RP with longer IS/OS lines had larger fmERG amplitudes.

However, we found that the correlation between the amplitude of the fmERGs and changes in the OCT image was weak, even when the integrity of the IS/OS line was used to separate the patients with RP into the three groups. The weak correlation was probably due to two factors: first, there was no statistically significant difference in the fmERG amplitude between types 2 and 3 ($P = 0.07$ for a-wave; $P = 0.20$ for b-wave); and second, there was a large variation in the amplitudes of the fmERGs in type 1 and some patients had severely reduced amplitudes (Fig. 5, bottom plot).

Patients with RP with Normal Macular Volume but Severely Reduced fmERGs

Finally, we wanted to investigate whether the IS/OS line was preserved in our four patients with normal macular volume and severely reduced fmERG amplitudes (Fig. 4). We expected that even though the total macular volume was within the normal range, these patients may have had a very short IS/OS line, which may be the reason for severely reduced mfERG. The gray-scale OCT images and the waveforms of fmERG in four patients with RP who had normal macular volume and severely reduced fmERG amplitude (patients 4–7) are shown

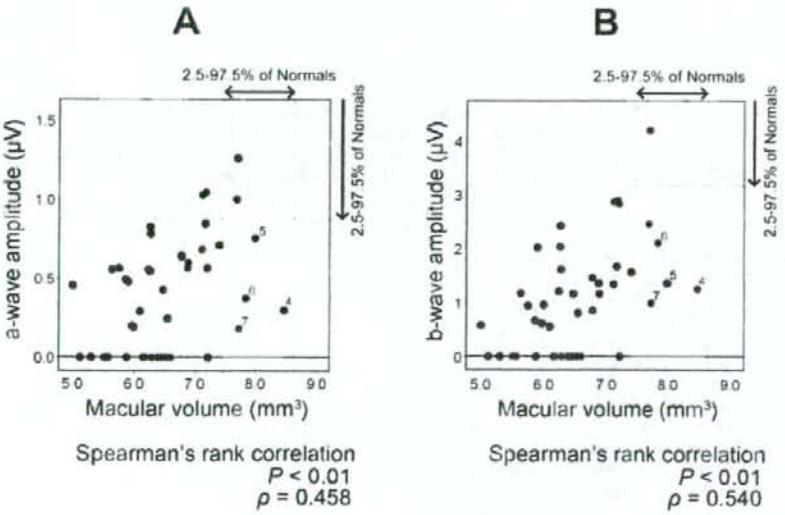

FIGURE 4. Amplitudes of a- and b-waves plotted against total macular volume in 43 patients with RP. There is a weak but significant correlation between the fmERG amplitude and total macular volume. There were four patients with RP who had normal macular volume but severely reduced fmERG (patients 4–7). *Shaded area*: the 2.5 to 97.5 percentiles of total macular volume and mfERG amplitude in age-similar normal subjects.

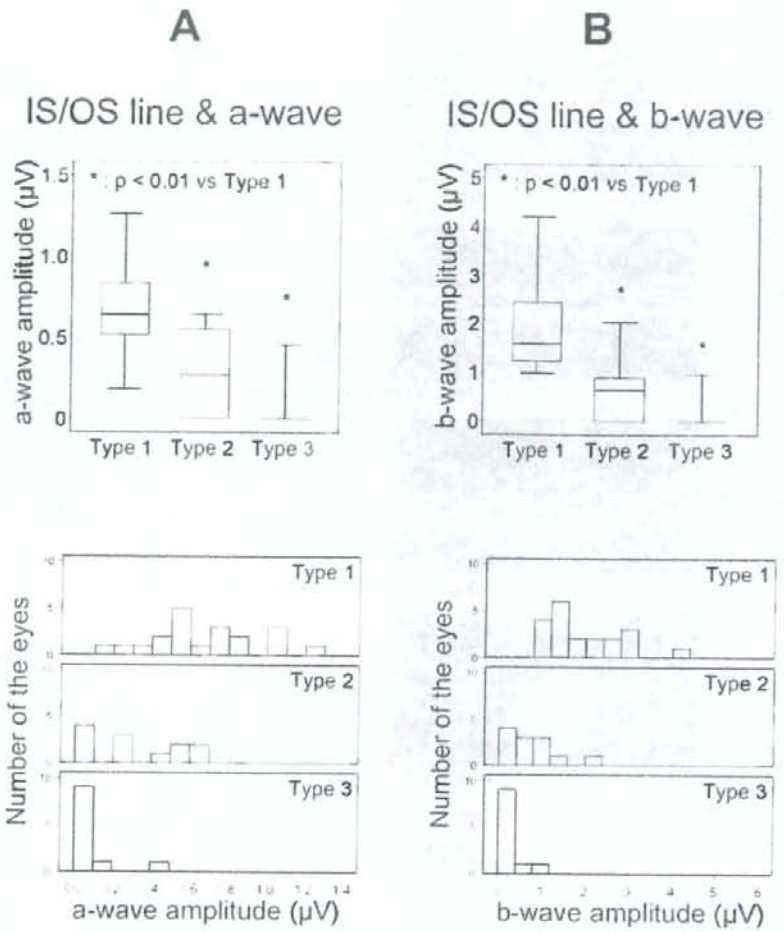

FIGURE 5. The (A) a- and (B) b-wave amplitudes of the fmERGs for patients with RP with the three types of IS/OS line configuration (see also Fig. 1). *Top*: The fmERG amplitudes in type 1 patients with RP were significantly larger than those in type 2 or 3 patients with RP. *Bottom*: histograms of the fmERG amplitude for three types of patients with RP.

in Figure 6. Against our expectations, the length of IS/OS line was relatively well-preserved (>4 mm) for these four patients, and was more than 5 mm for three patients (patients 4, 5, and 7). These results indicated that there are some patients with RP whose total macular volume and the length of IS/OS line were relatively well preserved in the macular area, but their electrophysiological function within this area was severely affected.

DISCUSSION

Our results demonstrated that there was a significant correlation between the amplitudes of the a- and b-waves of the fmERG and the total macular volume in our 43 patients with RP. These results were not surprising because the gradual thinning of the retina caused by the shortening of outer segments and the loss of photoreceptors should result in the reduction of the fmERG amplitude in the retina of patients with RP. The results of an earlier study on the correlation between the retinal histopathology and ERG findings in an animal model of RP support this idea.[52]

Although there was a significant correlation between the amplitude of the fmERG and total macular volume, the degree of correlation was weak: the coefficient of correlation (ρ) was only 0.46 for the a-wave, and 0.54 for the b-wave. One of the major reasons for this weak correlation was that there were four patients with RP who had normal macular volume but severely reduced fmERG amplitudes (Fig. 4). In contrast, there were no patients with RP who had normal fmERG amplitude but severely reduced total macular volume. These results indicate that a normal total macular volume does not guarantee normal electrophysiological function of the macula in patients with RP.

We initially reasoned that the weak correlation might be because we used total macular volume as a measure of macular structure. It is well known that the early histopathologic changes in eyes of patients with RP were mainly a shortening or distortion of the rod and cone photoreceptors.[6–8] Thus, we next investigated whether the structural integrity of the IS/OS junction (i.e., the length of the IS/OS line) correlated with the amplitude of the fmERG. As shown, the length of the IS/OS line generally correlated with the fmERG amplitude. However, the correlation between the length of IS/OS line and the fmERG amplitude was also weak. Careful examinations of the OCT images and fmERG records in individual patients with RP

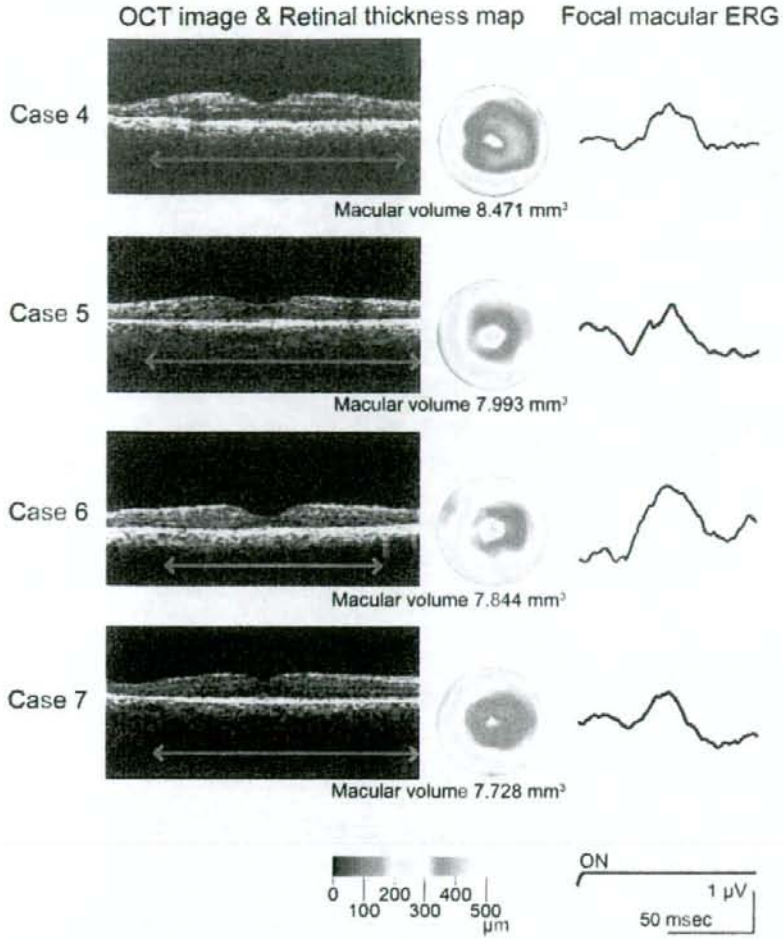

FIGURE 6. Gray-scale OCT images and fmERGs recorded in four patients with RP who had normal macular volume but severely reduced fmERG (see also Fig. 4). *Red lines*: the length of detectable IS/OS lines on the gray-scale OCT images. The amplitudes of fmERGs were severely reduced in all four patients, but the length of the IS/OS line was more than 4 mm in all patients and was more than 5 mm in three of five patients.

showed that there were four patients with RP who had normal macular volume and a relatively long IS/OS line, but severely reduced fmERG amplitudes (Fig. 6). Of interest, three of these four patients had a detectable IS/OS line longer than 5 mm. These results indicated that there are some patients with RP whose macular OCT images are relatively well preserved, but their electrophysiological functions are severely reduced.

The exact reason that some patients with RP had a preserved macular OCT image but severely reduced fmERG was not determined. There are two possibilities: First, these patients may have very subtle structural changes, but our OCT system (third-generation Stratus OCT) may not have detected the changes. For example, using ultrahigh-resolution OCT, Witkin et al.[30] measured the distance between the IS/OS line and the outer border of the retinal pigment epithelium thickness (called FOSPET), and demonstrated an excellent correlation between visual acuity and FOSPET in nine patients with RP. In our study, we were able to measure the length of the IS/OS line, but could not obtain reliable measurements of FOSPET in our OCT images. New-generation, high-resolution OCT instruments may enable us to make these measurements.

A second possibility is that the functional abnormality may precede structural changes in the macula of some patients with RP. It was recently demonstrated that some patients with Leber congenital amaurosis (LCA), the most common inherited cause of blindness in childhood, can retain the cone photoreceptors and inner retinal architecture in the central retina, but have severely reduced central vision at a relatively early stage of the disease.[29,31] If this second possibility is correct, the combined assessment of macular structure by OCT and macular function by psychophysics or electrophysiology can provide important information on the macula of patients with RP.

There are some limitations in our study. First, we planned to measure the volume of the inner, middle, and outer retinal layers separately and wanted to examine the correlation between the volumes in each layer and the fmERG amplitude. This comparison was possible in normal subjects, but was difficult in patients with RP with severely reduced macular thickness. Recent advances in new ultrahigh-resolution OCT technique may enable analysis of the thickness of each retinal layer, and this will allow us to investigate the changes in each retinal layer after photoreceptor degenerations. Second, we investigated the correlation of macular volume with the fmERG amplitude, but did not study the correlation with the implicit time, because there were many patients with RP whose amplitude of fmERG was so reduced that the implicit time could not

be measured precisely. However, the correlation between the implicit time and OCT images may be interesting, because the results of past studies have shown that the delay in the implicit time of focal ERGs can be another important indicator of functional changes in the macula area of patients with RP.[14–19] Third, we did not record the OCT and mfERGs from the same patient at different time points, and thus cannot examine the longitudinal progression of the changes in patients with RP.

In conclusion, we studied the correlation between the fmERG amplitude and macular structure by OCT and found that there was a significant correlation between these two measures, but the degree of correlation was weak. One major reason for this low correlation was the presence of some patients with RP who had well-preserved macular OCT images but severely reduced fmERGs. Although the exact mechanism for this discrepancy needs further investigation, we believe that the combined examination of macular structure by OCT and macular function by fmERG can provide important information on the pathophysiology, prognosis, and future treatments in patients with RP.

References

1. Carr RE, Heckenlively JR. Hereditary pigmentary degenerations of the retina. In: Duane TD, Jaeger EA, eds. *Clinical Ophthalmology*. Philadelphia: JB Lippincott; 1987;1–28.
2. Heckenlively JR. RP syndromes. In: Heckenlively JR, ed. *Retinitis Pigmentosa*. Philadelphia: JB Lippincott; 1988;221–252.
3. Newsome DA. Retinitis pigmentosa, Usher's syndrome, and other pigmentary retinopathies. In: Newsome DA, ed. *Retinal Dystrophies and Degenerations*. New York: Raven Press; 1988;161–194.
4. Weleber RG, Gregory-Evance K. Retinitis pigmentosa and allied disorders. In: Hinton DR, ed. *Retina*. 4th ed. Vol. 1. Basic science and inherited retinal disease. St. Louis: Mosby; 2006;395–498.
5. Hartong DT, Berson EL, Dryja TP. Retinitis pigmentosa. *Lancet*. 2006;368:1795–1809.
6. Szamier RB, Berson EL, Klein R, Meyers S. Sex-linked retinitis pigmentosa: ultrastructure of photoreceptors and pigment epithelium. *Invest Ophthalmol Vis Sci*. 1979;18:145–160.
7. Milam AH, Li ZY, Fariss RN. Histopathology of the human retina in retinitis pigmentosa. *Prog Retin Eye Res*. 1998;175–205.
8. Fariss RN, Li ZY, Milam AH. Abnormalities in rod photoreceptors, amacrine cells, and horizontal cells in human retinas with retinitis pigmentosa. *Am J Ophthalmol*. 2000;129:215–223.
9. Sandberg MA, Effron MH, Berson EL. Focal cone electroretinograms in dominant retinitis pigmentosa with reduced penetrance. *Invest Ophthalmol Vis Sci*. 1978;17:1096–1101.
10. Biersdorf WR. Temporal factors in the foveal ERG. *Curr Eye Res*. 1982;1:717–722.
11. Seiple W, Siegel IM, Carr RE, Mayron C. Evaluating macular function using the focal ERG. *Invest Ophthalmol Vis Sci*. 1986;27:1123–1130.
12. Falsini B, Iarossi G, Porciatti V, et al. Postreceptoral contribution to macular dysfunction in retinitis pigmentosa. *Invest Ophthalmol Vis Sci*. 1994;35:4282–4290.
13. Ikenoya K, Kondo M, Piao CH, et al. Preservation of macular oscillatory potentials in eyes of patients with retinitis pigmentosa and normal visual acuity. *Invest Ophthalmol Vis Sci*. 2007;48:3312–3317.
14. Hood DC, Holopigian K, Greenstein V, et al. Assessment of local retinal function in patients with retinitis pigmentosa using the multi-focal ERG technique. *Vision Res*. 1998;38:163–179.
15. Chan HL, Brown B. Investigation of retinitis pigmentosa using the multifocal electroretinogram. *Ophthalmic Physiol Opt*. 1998;18:335–350.
16. Seeliger MW, Kretschmann UH, Apfelstedt-Sylla E, Zrenner E. Implicit time topography of multifocal electroretinograms. *Invest Ophthalmol Vis Sci*. 1998;39:718–723.
17. Felius J, Swanson WH. Photopic temporal processing in retinitis pigmentosa. *Invest Ophthalmol Vis Sci*. 1999;40:2932–2944.
18. Hood DC. Assessing retinal function with the multifocal technique. *Prog Retin Eye Res*. 2000;19:607–646.
19. Holopigian K, Seiple W, Greenstein VC, et al. Local cone and rod system function in patients with retinitis pigmentosa. *Invest Ophthalmol Vis Sci*. 2001;42:779–788.
20. Vajaranant TS, Seiple W, Szlyk JP, Fishman GA. Detection using the multifocal electroretinogram of mosaic retinal dysfunction in carriers of X-linked retinitis pigmentosa. *Ophthalmology*. 2002;109:560–568.
21. Robson AG, Saihan Z, Jenkins SA, et al. Functional characterization and serial imaging of abnormal fundus autofluorescence in patients with retinitis pigmentosa and normal visual acuity. *Br J Ophthalmol*. 2006;90:472–479.
22. Jacobson SG, Buraczynska M, Milam AH, et al. Disease expression in X-linked retinitis pigmentosa caused by a putative null mutation in the RPGR gene. *Invest Ophthalmol Vis Sci*. 1997;38:1983–1997.
23. Jacobson SG, Cideciyan AV, Huang Y, et al. Retinal degenerations with truncation mutations in the cone-rod homeobox (CRX) gene. *Invest Ophthalmol Vis Sci*. 1998;39:2417–2426.
24. Jacobson SG, Cideciyan AV, Iannaccone A, et al. Disease expression of RP1 mutations causing autosomal dominant retinitis pigmentosa. *Invest Ophthalmol Vis Sci*. 2000;41:1898–1908.
25. Schatz P, Abrahamson M, Eksandh L, Ponjavic V, Andréasson S. Macular appearance by means of OCT and electrophysiology in members of two families with different mutations in RDS (the peripherin/RDS gene). *Acta Ophthalmol Scand*. 2003;81:500–507.
26. Jacobson SG, Cideciyan AV, Aleman TS, et al. Crumbs homolog 1 (CRB1) mutations result in a thick human retina with abnormal lamination. *Hum Mol Genet*. 2003;12:1073–1078.
27. Sandberg MA, Brockhurst RJ, Gaudio AR, Berson EL. The association between visual acuity and central retinal thickness in retinitis pigmentosa. *Invest Ophthalmol Vis Sci*. 2005;46:3349–3354.
28. Schwartz SB, Aleman TS, Cideciyan AV, et al. Disease expression in Usher syndrome caused by VLGR1 gene mutation (USH2C) and comparison with USH2A phenotype. *Invest Ophthalmol Vis Sci*. 2005;46:734–743.
29. Jacobson SG, Aleman TS, Cideciyan AV, et al. Identifying photoreceptors in blind eyes caused by RPE65 mutations: prerequisite for human gene therapy success. *Proc Natl Acad Sci USA*. 2006;102:6177–6182.
30. Witkin AJ, Ko TH, Fujimoto JG, et al. Ultra-high resolution optical coherence tomography assessment of photoreceptors in retinitis pigmentosa and related diseases. *Am J Ophthalmol*. 2006;142:945–952.
31. Cideciyan AV, Aleman TS, Jacobson SG, et al. Centrosomal-ciliary gene CEP290/NPHP6 mutations result in blindness with unexpected sparing of photoreceptors and visual brain: implications for therapy of Leber congenital amaurosis. *Hum Mutat*. 2007;28:1074–1083.
32. Jacobson SG, Cideciyan AV, Aleman TS, et al. Leber congenital amaurosis caused by an RPGRIP1 mutation shows treatment potential. *Ophthalmology*. 2007;114:895–898.
33. Aleman TS, Cideciyan AV, Sumaroka A, et al. Inner retinal abnormalities in X-linked retinitis pigmentosa with RPGR mutations. *Invest Ophthalmol Vis Sci*. 2007;48:4759–4765.
34. Apushkin MA, Fishman GA, Alexander KR, Shahidi M. Retinal thickness and visual thresholds measured in patients with retinitis pigmentosa. *Retina*. 2007;27:349–357.
35. Walia S, Fishman GA, Edward DP, Lindeman M. Retinal nerve fiber layer defects in RP patients. *Invest Ophthalmol Vis Sci*. 2007;8:4748–4752.
36. Matsuo T, Morimoto N. Visual acuity and perimacular retinal layers detected by optical coherence tomography in patients with retinitis pigmentosa. *Br J Ophthalmol*. 2007;91:888–9033.
37. Horio N, Kachi S, Hori K, et al. Progressive change of optical coherence tomography scans in retinal degeneration slow mice. *Arch Ophthalmol*. 2001;119:1329–1332.
38. Li Q, Timmers AM, Hunter K, et al. Noninvasive imaging by optical coherence tomography to monitor retinal degeneration in the mouse. *Invest Ophthalmol Vis Sci*. 2001;42:2981–2989.

39. Huang Y, Cideciyan AV, Papastergiou GI, et al. Relation of optical coherence tomography to microanatomy in normal and rd chickens. *Invest Ophthalmol Vis Sci.* 1998;39:2405–2416.
40. Huang Y, Cideciyan AV, Alemán TS, et al. Optical coherence tomography (OCT) abnormalities in rhodopsin mutant transgenic swine with retinal degeneration. *Exp Eye Res.* 2000;70:247–251.
41. Marmor MF, Holder GE, Seeliger MW, Yamamoto S; International Society for Clinical Electrophysiology of Vision. Standard for clinical electroretinography (2004 update). *Doc Ophthalmol.* 2004; 108:107–114.
42. Miyake Y, Shiroyama N, Ota I, Horiguchi M. Oscillatory potentials in electroretinograms of the human macular region. *Invest Ophthalmol Vis Sci.* 1988;29:1631–1635.
43. Miyake Y. Studies of local macular ERG (in Japanese). *Acta Soc Ophthalmol Jpn.* 1988;92:1418–1449.
44. Wong TY, Foster PJ, Ng TP, et al. Variations in ocular biometry in an adult Chinese population in Singapore: the Tanjong Pagar Survey. *Invest Ophthalmol Vis Sci.* 2001;42:73–80.
45. Shufelt C, Fraser-Bell S, Ying-Lai M, et al. Refractive error, ocular biometry, and lens opalescence in an adult population: the Los Angeles Latino Eye Study. *Invest Ophthalmol Vis Sci.* 2005;46: 4450–4460.
46. Olsen T, Arnarsson A, Sasaki H, et al. On the ocular refractive components: the Reykjavik Eye Study. *Acta Ophthalmol Scand.* 2007;85:361–366.
47. Costa RA, Calucci D, Skaf M, et al. Optical coherence tomography 3: Automatic delineation of the outer neural retinal boundary and its influence on retinal thickness measurements. *Invest Ophthalmol Vis Sci.* 2004;45:2399–2406.
48. Ishikawa K, Kondo M, Ito Y, et al. Correlation between focal macular electroretinograms and angiographic findings after photodynamic therapy. *Invest Ophthalmol Vis Sci.* 2007;48:2254–2259.
49. Drexler W, Sattmann H, Hermann B, et al. Enhanced visualization of macular pathology with the use of ultrahigh-resolution optical coherence tomography. *Arch Ophthalmol.* 2003;121:695–706.
50. Costa RA, Skaf M, Melo LA Jr, et al. Retinal assessment using optical coherence tomography. *Prog Retin Eye Res.* 2006;25:325–353.
51. Pons ME, and Garcia-Valenzuela E. Redefining the limit of the outer retina in optical coherence tomography scans. *Ophthalmology.* 2005;112:1079–1085.
52. Machida S, Kondo M, Jamison JA, et al. P23H rhodopsin transgenic rat: correlation of retinal function with histopathology. *Invest Ophthalmol Vis Sci.* 2000;41:3200–3209.

液晶視力表　システムチャート SC-2000の臨床評価

Clinical evaluation of liquid crystal displayed visual acuity test "System chart SC-2000"

浅野麻衣[1*]・正木勢津子[1]・稲垣理佐子[1]・彦谷明子[1]・堀田喜裕[1]・佐藤美保[1]

Mai Asano[1*]・Setsuko Masaki[1]・Risako Inagaki[1]・Akiko Hikoya[1]・Yoshihiro Hotta[1]・Miho Sato[1]

【要約】 日常診療では種々の視力表が用いられている．しかし，それらは視標背景の輝度のばらつきが大きく，また，標準化されているとはいえない．今回，プロトタイプの液晶視力検査装置がニデック社によって作製された．我々は，①液晶視力表システムチャートSC-2000®と従来の視力検査装置の視力の比較と，②SC-2000の液晶モニターを斜めから見たときの視力への影響の2点から臨床的に評価した．

その結果，SC-2000は，従来から用いられている准標準視力検査装置と有意差なく，相関のある視力結果が得られた．視標正面から15°以内の測定位置のずれであれば，正面から見ているのと同等の視力が得られた．ハロゲンランプを光源とし，1視標につきランプ1つか2つで後方から照らす従来の視力検査装置に比べ，安定した条件で検査が可能であり，多施設で視力の比較をする場合，共通の視力検査装置として使用可能であると考えた．

【キーワード】 液晶視力検査装置，准標準視力検査表，液晶モニター，背景輝度，視力

緒言

我が国で用いられている視力検査装置は，標準視力検査装置と准標準視力検査装置，特殊視力検査装置の3種類に分けられる．JIS規格の中で，標準視力検査装置は，輝度が80～320cd/m^2，コントラストが74％以上で，視標には8方向のランドルト環を用いることが必要と規定している．また，視力値の段階はlog MARステップを用い，視標の精度は1.6までは標準値の±5％，2.0は±10％以内であるほか，最小視標数，視標相互の間隔なども細かく規定され，視標の背景は均一で明るく見えること，という条件がついている．准標準視力検査装置は，遠距離視力検査用に作製されたもので，ランドルト環およびランドルト環と相関づけられた視標を用い，実用性に重点をおく装置とされている．視標の精度は標準値の±10％以内である．また，特殊視力検査装置は，近距離視力検査装置，字ひとつ視力検査装置，スクリーニング用視力検査装置，両眼開放視力検査装置，光学式視力検査装置などを含み，ランドルト環およびランドルト環と相関づけられた視標を用いた装置である．精度は准標準視力検査装置と同じく±10％以内であるが，同一段階の視標数に特に定めはない[1-3]．これに従うと日常診療で広く用いられている視力検査装置は，准標準視力検査装置と特殊視力検査装置である．

我々は，液晶モニターの特徴を調べるために，従来使用している准標準視力検査装置を用い，視標の背景輝度の比較を行った．図1に示すように，0.1の視標の周囲5ヵ所を選択して，液晶モニターおよび従来型の2機種の准標準視力検査装置を比較した．視標の背景輝度のばらつきは，従来の背景照明を用いる視力検査装置では大きく，液晶モニターでは小さいことが明らかであった(表1)．

1 浜松医科大学眼科 Department of Ophthalmology, Hamamatsu University School of Medicine

＊別刷請求先 431-3192 静岡県浜松市東区半田山1-20-1
浜松医科大学眼科 浅野麻衣

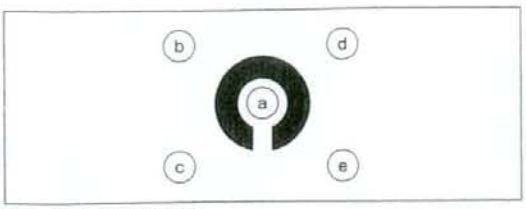

図1　背景輝度の測定場所
0.1の視標の周囲5ヵ所を，液晶モニターおよび従来型の2機種の准標準視力検査装置で測定した．

表1　視力表による背景輝度の比較

	a	b	c	d	e
液晶視力表（実験機）	299.5	284.6	281.6	294.8	293.7
A社製：准標準視力検査表	328.5	214.8	201.4	231.7	210.3
B社製：准標準視力検査表	337.8	239.9	227.1	217.7	230.9

米国を中心とした弱視に関する多施設共同研究では，コンピュータで制御された視標をCRTあるいは液晶モニター上に表示する電子視力検査装置が開発され，研究のための共通の検査装置として用いられている．一方，我が国では，そのような視力検査装置が研究目的で用いられているものの市販はされていない．そのため，標準化された視力検査装置が必要であると考えた．コンピュータ制御を行うことで，1つのモニターで，准標準視力検査だけでなく，字ひとつ視力検査，字多数視力検査，コントラスト感度検査といった様々な視力評価を行う可能性がでてくる．近年の液晶モニターの高輝度化，および価格低下によって，液晶モニターを用いた視力検査装置の普及の可能性が高くなった，我々はその開発に協力をしてきた．

今回，プロトタイプの液晶視力検査装置がニデック社によって作製されたため，使用上の問題点を探るために以下の検討を行った．

①液晶視力表 システムチャート SC-2000® (以下；SC-2000) と従来の視力検査装置の視力の比較と，②SC-2000の液晶モニターを斜めから見たときの視力への影響の2点から臨床的に評価したので報告する．

対象および方法

SC-2000の液晶モニターは，19インチ（高解像度SXGA液晶），解像度1280×1024，1ドットが0.294×0.294mmであり，動作は産業用マイクロプロセッサーで行われる．視標は，0.03～0.05までは1つ，0.06～0.08までは2つ，0.1，0.15は3つ，0.2より小さい場合には5つ，が同時に1画面に提示される．視標は小数視力を用いている．提示はリモートコントロールによって変化させることが可能である．

1．SC-2000と従来の視力検査装置との視力の比較

視標の表示方法は，SC-2000ではモニターに提示可能な視標数に制限があるため，今回の比較では字ひとつ表示を用いた．比較に用いた検査装置には，従来から広く用いられている字づまり表示のA社製准標準視力検査装置を使用した．これは，視標を，A12V，5Wのハロゲンランプで後方から照らすものである．

対象は，屈折異常以外に眼疾患のない20～50歳の成人20名40眼と，浜松医科大学眼科通院中で，同日に2機種での視力検査に協力が得られた，5～10歳の小児14名28眼とした．

測定方法は，集中力・疲労といった検査の順による視力への影響を考慮し，成人・小児とも半数ずつ，検査の順を変え測定した．検査距離5mで，同一検者が自覚的レンズ交換法による完全屈折矯正を行い測定し，60％以上の正解を視力値とした．そして2機種間での比較をWilcoxonの符号順位和検定で行い（$p < 0.05$ を有意差あり），さらに，相関を検討した．検査室の明るさは，JIS規格の遠距離視力検査方法の条件内であった．

2．SC-2000の液晶モニターを斜めから見たときの視力への影響

対象は，屈折異常以外に眼疾患のない成人5名10眼とした．

測定方法は，検査距離3mとし，視標サイズはその距離に設定変更して行った．そして，図2に示すように，液晶モニター正面を0°とし，モニター面に対して水平に5°間隔で15°までの4ヵ所で，同一検者が自覚的レンズ交換法による完全屈折矯正を行い測定し，60％以上の正解を視力値とした．このとき，15°の位置は正面0°の位置より約0.9m離れた位置となる．